pH-Dependent Phase Behavior of Carbohydrate-Based Gemini Surfactants. The Effects of Carbohydrate Stereochemistry, Head Group Hydrophilicity, and Nature of the Spacer

Jaap E. Klijn,[†] Marc C.A. Stuart, Marco Scarzello, Anno Wagenaar, and Jan B. F. N. Engberts*

Physical Organic Chemistry Unit, Stratingh Institute, University of Groningen, 9747 AG Groningen, The Netherlands

Received: February 16, 2007

The pH-dependent phase behavior and hydroxide-ion adsorption ability of a series of (reduced) carbohydrate-based gemini surfactants were studied between pH 2 and 12. Static and dynamic light scattering were employed to address transitions in the aggregate morphologies and cryo-electron microscopy was used to provide further evidence for the morphologies present in solution. Changes in aggregate structure as a result of a change in solution pH and an accompanying change in protonation state or a change in molecular structure can be rationalized in terms of the variations in the packing parameter. In this paper we have focused our attention on the size of the carbohydrate moiety, the carbohydrate stereochemistry and the nature of the spacer (hydrophobic vs hydrophilic). At near neutral pH, most of the gemini surfactants form vesicles. Upon lowering of the pH, the vesicles undergo a transition toward wormlike micelles followed by a transition to spherical micelles. Upon increasing the solution pH, flocculation occurs due to charge neutralization followed at still higher pH by redispersion and charge reversal of the vesicles through the specific adsorption of hydroxide ions to the vesicular surface. Upon decreasing head group size at constant, but low, degrees of protonation, the packing parameter has a tendency to become larger than one resulting in the formation of inverted phases. Upon further decrease in the head group size, oil droplets are observed. In case of a hydrophobic spacer, the carbohydrate stereochemistry affects the pH of the transitions, but not the type of the transitions. By contrast, for a hydrophilic spacer, the pH of the transitions remains unaffected. Adsorption of hydroxide ions at basic pH follows similar trends, but was only found for vesicles and oil droplets. The large range of structural variations that we have examined allows a better understanding of the requirements for the phase transitions for carbohydrate-based gemini surfactants as well as for the physisorption of hydroxide ions to interfaces in general.

Introduction

Surfactants are molecules that contain a hydrophilic head group attached to a large hydrophobic part. Typically, the hydrophobic part is an alkyl group with at least eight CH_2 units. The head group can be cationic, anionic, zwitterionic, or nonionic. Gemini (or dimeric) surfactants are obtained when two classical surfactants are covalently linked through a spacer.[1] The first gemini surfactants were synthesized in 1971 (Scheme 1A), and this class of gemini surfactants still represents the most commonly used gemini surfactants.[2] Their phase behavior in water has attracted considerable interest, since it is quite different from that of conventional surfactants. For example, their cmc values are one or 2 orders of magnitude smaller than those of their monomeric counterparts.[1] It is also possible to obtain wormlike micelles at low concentrations in the absence of additional salt.[3] For these and other reasons, industry has taken strong interest in these types of surfactants.

In the past years, the structures of gemini surfactants have been extensively varied by changing the spacer, head groups, tails,[1] and even by synthesizing gemini surfactants by combining two non-identical surfactants.[4,5] These surfactants usually carry charges independent of the solution pH, or are charged over a large pH range. In our laboratory a series of (reduced) carbohydrate-based gemini surfactants with two amine functionalities (Scheme 1B) has been investigated.[6−9] In these geminis the protonation state can be varied from zero to two in an easily accessible pH range. They were initially developed as nonviral gene-delivering vehicles, and promising results have been obtained both in vitro[10] and in vivo.[11] But also in the absence of DNA, they possess intriguing phase behavior. Aggregates observed, upon variation of the pH, include micelles, vesicles, oil droplets, and inverted phases. The presence of such a variety of aggregates is not exclusively the result of variation in pH, but can also be induced by a number of molecular variations in the gemini amphiphile structure.[6,7,9] Variations that have already been examined include the length of the hydrophobic spacer[9] and shortening or removal of the carbohydrate unit.[8,9] This latter effect induced, for example, the formation of

SCHEME 1: Structure of Commonly Used Gemini Amphiphiles; X^- is Cl^- or Br^- (A); General Structure of the Gemini Surfactants Used in this Study (B)

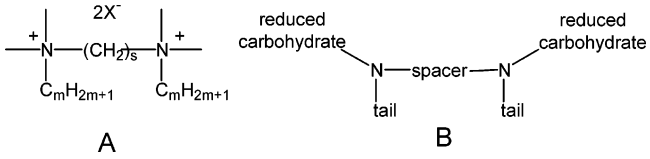

* Corresponding author. E-mail: J.B.F.N.Engberts@rug.nl.
[†] Present Address: Polymer Service Centre Groningen, Kadijk 7D, 9747 AT Groningen.

10.1021/jp071354g CCC: $37.00
Published on Web 04/18/2007

oil droplets instead of vesicles at near neutral pH. Also, the effect of carbohydrate stereochemistry and the nature of the spacer (hydrophobic versus hydrophilic)[7] have been briefly addressed.[7] It was found that the pH values of particular transitions, such as, for example, the wormlike-micelle-to-vesicle transition, can strongly depend on the molecular structure of the gemini surfactant. Intriguingly, it was also found that at high pH both vesicles and oil droplets adsorb hydroxide ions.[7−9]

In this paper we turned our attention to the effects of the size of the (carbohydrate) head group, the carbohydrate stereochemistry, the nature of the spacer on the pH-dependent phase behavior and the hydroxide-ion adsorption ability. The size of the (carbohydrate) head group was varied from one carbon atom to twelve. The spacer was varied from a hydrophobic *n*-hexyl spacer to a hydrophilic oligo ethylene oxide spacer. Finally, different (reduced) carbohydrates were used to study the effect of carbohydrate stereochemistry.

Experimental

Materials. Gemini surfactants were synthesized as described previously.[12] Detailed synthetic procedures will be reported in a forthcoming paper.[13] Hepes, Mes (4-morpholinoethanesulfonic acid), APS (3-amino-1-propanesulfonic acid), and taurine (2-aminoethanesulfonic acid) were purchased from Sigma and used as received.

Sample Preparation. Solutions of gemini surfactant in chloroform were dried under a stream of nitrogen. Traces of residual solvent were removed under vacuum. To obtain small unilamellar vesicles (SUVs) with a narrow and reproducible size distribution, the lipid films were hydrated at room temperature in bidistilled water containing 5 mM each of the buffer substances Hepes, Mes, and taurine and 10 mM of APS at a pH close to the pH of flocculation of the particular gemini surfactant being studied (unless stated otherwise), vortexed for several minutes, briefly tip-sonicated (<30 s), freeze-thawed [N_2(l) ↔ water bath (40 °C)] 5 times, and extruded 11 times through a 200-nm-pore-size polycarbonate filter. Typically, this procedure leads to vesicles with a maximum in the size distribution of about 150 nm.

The samples for light scattering measurements were prepared by diluting the 5 mM (total surfactant concentration) vesicular stock solutions to a final concentration of 0.25 mM and adding a few microliters of HCl (aq) (ca. 4 M) or NaOH (aq) (ca. 2M) to obtain the desired pH. The dispersions were allowed to equilibrate overnight before measuring.

Static and Dynamic Light Scattering. Static and dynamic light scattering measurements were performed at 25 °C on a Zetasizer 5000 instrument (Malvern Instruments, U.K.) at $\lambda = 633$ nm. To obtain the hydrodynamic radii, the intensity autocorrelation functions were analyzed using CONTIN. The obtained intensities from static light scattering experiments were normalized against the maximum scattered intensity for that particular gemini surfactant. The experimental data of duplo experiments was normalized such that the curves overlap and the pH of the transitions are most clearly displayed. Note that trends in scattered intensities are meaningful, but that absolute values of scattered intensities obtained solely from larger structures (vesicles, inverted phases) are relatively meaningless.

Cryo-Transmission Electron Microscopy. A drop of the lipid suspension was deposited on a glow discharged holey carbon-coated grid. After blotting away the excess of liquid, the grids were rapidly plunged into liquid ethane. The frozen specimens were mounted in a Gatan (model 626) cryo-stage and examined in a Philips CM 120 cryo-electron microscope operating at 120 kV. Micrographs were recorded under low-dose conditions.

TABLE 1: Overview of Gemini Surfactants Used in this Study

	head group[a]	position of hydroxy groups[b]	spacer
1	D-glucose	*R,S,R,R*	$-(EO)_2-(CH_2)_2-$
2	D-glucose	*R,S,R,R*	$-(CH_2)_6-$
3	D-arabinose	*S,R,R*	$-(CH_2)_6-$
4	D-erithrose	*R,R*	$-(CH_2)_6-$
5	D,L-glycerol	racemic	$-(CH_2)_6-$
6	methyl		$-(CH_2)_6-$
7	D-lactose	1β-gal-4-glu[c]	$-(CH_2)_6-$
8	D-melibiose	1α-gal-6-glu[c]	$-(CH_2)_6-$
9	D-mannose	*S,S,R,R*	$-(CH_2)_6-$
10	D-mannose	*S,S,R,R*	$-(EO)_2-(CH_2)_2-$
11	D-talose	*S,S,S,R*	$-(CH_2)_6-$
12	D-galactose	*R,S,S,R*	$-(CH_2)_6-$
13	D-galactose	*R,S,S,R*	$-(EO)_2-(CH_2)_2-$
14	D-lactose	1β-gal-4-glu[c]	$-(EO)_2-(CH_2)_2-$
15	D-glucose	*R,S,R,R*	$-CH_2-(EO)_5-(CH_2)_3-$

[a] In fact, the head groups are reduced carbohydrates. [b] Stereochemistry at the 2, 3, 4, and 5 position, respectively (Scheme 2). [c] Disaccharides formed from glucose and galactose. Lactose: β-gal is linked at the 1 position to the 4 position of glucose. Melibiose: α-gal is linked at the 1 position to the 6 position of glucose.

Results and Discussion

Structural Variations. Previously, the phase behavior of **1** (Table 1) has been studied by static and dynamic light scattering.[7] Phase transitions were confirmed by cryo-electron microscopy. **1** has a reduced glucose head group and a hydrophilic $-(EO)_2-(CH_2)_2-$ spacer. Morphological transitions were explained by considering the packing parameter *P*, introduced by Israelachvili and Ninham:[14]

$$P = \frac{V}{a_0 l_c} \tag{1}$$

In this equation V is the volume of the hydrophobic part of the molecule, a_0 the mean cross sectional head group surface area, and l_c the length of the extended all-trans alkyl tail. For a small packing parameter ($<1/3$), the shape of the surfactant favors a large positive curvature, leading to small aggregates (micelles). Between $1/3$ and $1/2$ wormlike micelles are usually observed and vesicles are formed when the packing parameter is between $1/2$ and 1. In case of a packing parameter that is larger than one, there is a negative curvature leading to inverted structures (e.g., hexagonal, cubic, etc.). We will use the term "relative packing parameter" when gemini surfactants are compared to one another at the same degree of protonation in order to be able to distinguish this situation from changes in the packing parameter resulting from changes in the degree protonation.

In the present study, **2** with a (reduced) glucose head group and a hydrophobic $(CH_2)_6-$ spacer, instead of a hydrophilic spacer, will be taken as a starting point for the present structural variations that we have examined. Table 1 shows the different gemini amphiphiles. For consistency with previous studies, where the tails were chosen such that flexible bilayers were formed, oleyl chains were selected as tails for all gemini surfactants.

The morphologies of the aggregates formed from the gemini surfactants were studied by static and dynamic light scattering and by cryo-electron microscopy. Vesicles formed from **2** can be prepared between pH 7.2 and 8.2 (Figure 1A). Decreasing

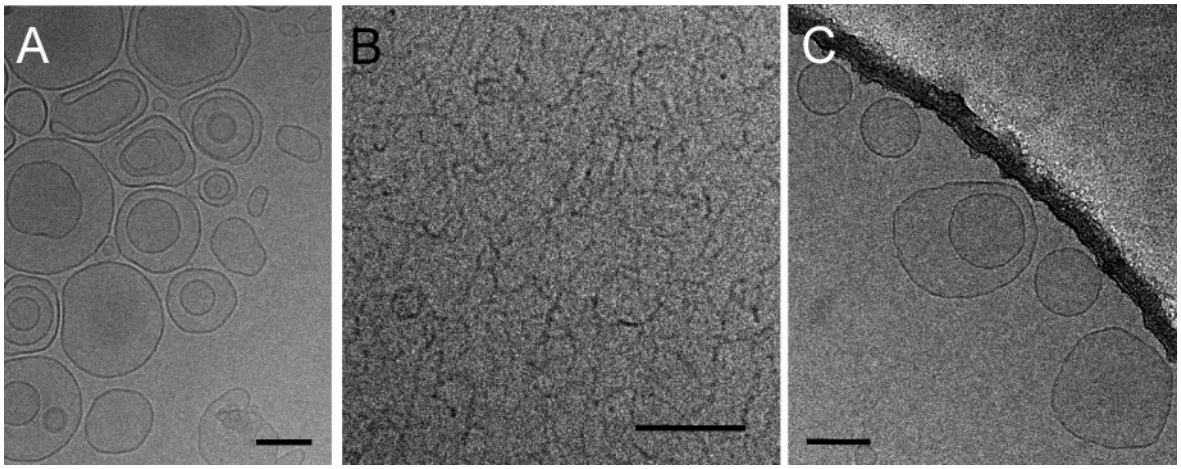

Figure 1. Cryo-electron microscopy pictures of **2** at pH 7.8 (A), 5.5 (B), and 11.8 (C). Bar represents 100 nm.

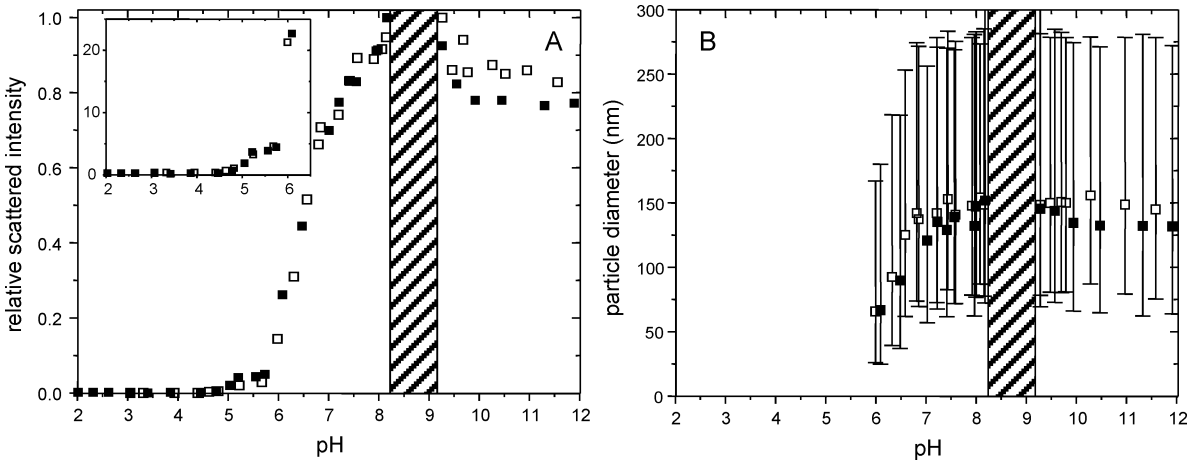

Figure 2. Relative scattered intensity (A) and size distributions (B) of solutions containing gemini surfactant **2** as a function of pH. Error bars denote the width of the size distribution.[1] Different symbols represent independent experiments starting from stock solutions prepared near neutral pH. The lined bar denotes the pH region where data could not be obtained due to flocculation. The insert in A displays the absolute scattered intensity.

the pH leads to a higher degree of protonation of the amine groups. As a result, the surface area increases (the packing parameter decreases), and wormlike micelles are formed that initially coexist with the remaining vesicles. The transition is accompanied by a strong decrease in the intensity of scattered light and a decrease of the maximum in the observed size distribution (Figure 2). At pH 5.9 the conversion is completed as evidenced by a low but constant scattering intensity (Figures 1B and 2A). At pH 4.6 the wormlike micelles are transformed into spherical micelles and the scattering intensity finally drops to a value close to that of the background signal. At this stage probably both nitrogen atoms are largely protonated,[12] and hence the smallest packing parameter is obtained.

Upon going in the opposite direction (i.e., pH 8.2), the electrostatic repulsion between the vesicles is lowered leading to flocculation. However, at pH 9.2 the vesicles redisperse with the same size distribution as before flocculation due to specific adsorption of hydroxide ions (Figures 1C and 2B).[12,15]

Effects of the Number of Hydroxy Groups in the Head Group. As a first structural variation the effects of the number of hydroxy group in the (reduced) carbohydrate on the phase behavior of the gemini surfactants was studied by stepwise removing the CH(OH) unit closest to the nitrogen atom from the carbohydrate of **2**. Of course, for the smaller head groups one can no longer consider the head group as a carbohydrate. The carbohydrate head group was also increased in size by attaching a galactose unit to the glucose group of **2**. In Figure 3 the pH of the transitions are shown as a function of the number of carbon atoms in the carbohydrate moiety. Figure 3 was obtained by combining plots of static and dynamic light scattering (Supporting Information and literature[8]) with cryo-electron microscopy pictures as was done previously.[9] Before addressing low pH transitions (pH $<$ 6), transitions associated with low degrees of protonation of the amine functionalities will be discussed.

Decreasing the size of the carbohydrate head group from six to five carbon atoms (**3**) leads to unexpected results. At pH 8.2 cryo-electron microscopy pictures (Figure 4A) show vesicles, some of which have invaginations and other irregular shapes at the surface of the vesicles. Similar structures have been reported previously and were identified as an L_3 phase, an intermediate phase in the transition from lamellar to inverted hexagonal[16] and cubic phases.[17] At pH 8.4 a phase transition toward micrometer long fibers is observed (Figure 4B and Supporting Information). Considering the near-linearity of the fibers (at least compared to the curvature in vesicles) at this pH, the gemini surfactants have probably a packing parameter of around 1. At pH $>$8.8 macroscopic phase separation occurs.

When the size of the carbohydrate head group is further decreased **4** is obtained. Up to pH 8.3 the static and dynamic light scattering data closely resemble those of both **2** and **3**. However, at pH $\geq$ 8.3 the solutions became progressively more turbid until macroscopic phase separation occurred at pH 8.9. Cryo-electron microscopy pictures were taken at pH 7.8 and

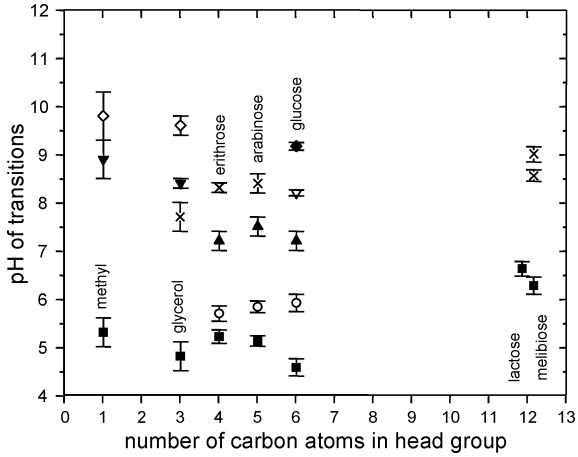

Figure 3. Plot of the pH of the transitions as a function of the number of carbon atoms in the head group. ▲ indicates the pH at which wormlike micelle formation from vesicles starts, ○ indicates the pH at which the formation of spherical micelles from wormlike micelles starts, ■ indicates the highest pH at which only spherical micelles are observed, ▽ indicates the pH of flocculation, ◆ indicates the pH of vesicle redispersion, ▼ indicates the pH of phase separation, ◇ indicates the pH of redispersion of oil droplets, and × indicates a transition not otherwise specified (see text for explanation).

8.6 (Figure 5A,B). At pH 7.8 similar structures as for **3** at pH 8.2 are observed (Figure 4A), while at pH 8.6 inverted, probably cubic,[17] structures can be seen (Figure 5B).

The formation of inverted phases at basic pH (low surface potential) is a result of a packing parameter larger than 1. Since the hydrophobic volume and length of the alkyl tails remain constant upon decreasing size of the carbohydrate moiety, the increase in the relative packing parameter must come from a decrease in the cross-sectional head group area of **4** as compared with those of **2** and **3**. Indeed, it is reasonable that at low surface potentials upon going from **2** to **4** the surface area of the gemini head groups at the same degree of protonation decreases.[9] Consistently, under these conditions **2, 3** and **4** form vesicles ($P < 1$), long fibers ($P =$ ca. 1) and an inverted phase ($P > 1$), respectively.

A further decrease in the size of the head group of **4** gives a gemini surfactant with a glycerol head group (**5**), of which the phase behavior has been briefly described recently.[8] In the same paper the phase behavior of the gemini surfactant with a methyl substituent at the nitrogen atoms has been described (**6**).

At low pH, **6** forms spherical micelles, but upon an increase in pH some of the initially charged gemini surfactant become neutral. Due to the low difference in polarity between the tails and the head group of the electrically neutral surfactant (which is liquid at room temperature), the gemini surfactant then enters the core of the micelle leading to the formation of oil droplets as evidenced by cryo-electron microscopy. With increasing pH they grow as more surfactant becomes oil and less surfactant remains to stabilize the droplets, until at pH 8.9, phase separation occurs. At pH 9.8 redispersion is observed due to adsorption of hydroxide ions and with increasing pH the droplets become smaller in size.[8]

5 is as an intermediate case between **6** and **4**, not only structurally, but also as far as the phase behavior is concerned. At room temperature **5** is a liquid, like **6**. However, when cryo-electron microscopy pictures are taken at pH 6.9 (Figure 5C) besides a few oil droplets, aggregates similar as those observed for **3** at pH 8.6 (Figure 4A) and **4** at pH 7.8 (Figure 5A) can be seen. Therefore, it seems likely that **5** also has a tendency to form inverted phases. However, **5** is apparently not able to form a stable inverted phase.

Due to the fact that the head group of unprotonated **6** is expected to be smaller than that of **5**, we speculate that inverted phases are not observed because the corresponding decrease in head group area is accompanied by a decrease in the polarity of the head group and sufficient to lead to oil droplet formation. Therefore, the transition at pH 5.3 can be compared to the transitions of **5** to **3** at pH 7.7, 8.3, and 8.6, respectively. Although the transitions are related to different phenomena, they have the same molecular origin. In line with expectations, starting from **6**, with increasing head group size (decreasing relative packing parameter) the pH at which aggregates with a packing parameter of one or larger are formed, requires a lower degree of protonation.

For **2** to **6** the highest pH at which only spherical micelles are present varies between 5.3 and 4.6. This is a relatively narrow pH range considering the increase in size of the carbohydrate moiety. Hence, it can be concluded that at low pH (1) the degree of protonation is only weakly affected by the size of the carbohydrate moiety and (2) the charged nitrogen atoms mainly determine the mean cross sectional head group area (and hence the packing parameter).[18] On the contrary, for **7** and **8** with a lactose and melibiose head group, respectively, this is no longer true (Figure 3) as the highest pH at which only spherical micelles are present increases to about 6.5. Hence, under these circumstances most likely the disaccharides are more important in determining the mean cross-sectional head group

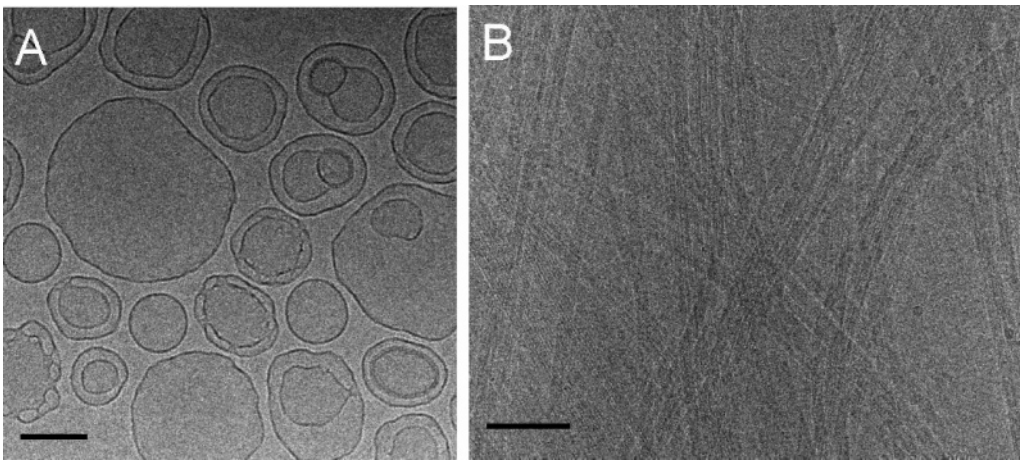

Figure 4. Cryo-electron microscopy pictures of **3** at pH 8.2 (A) and pH 8.6 (B). Bar represents 100 nm.

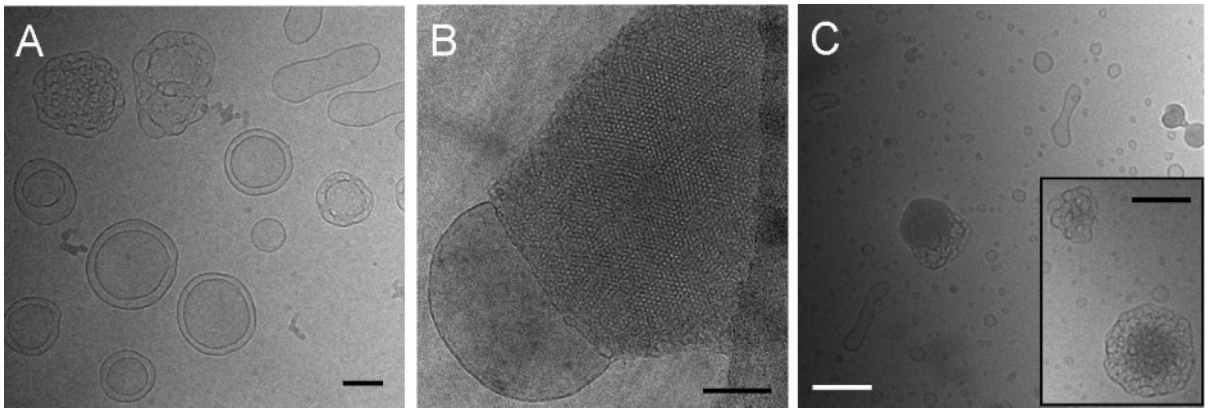

Figure 5. Cryo-electron microscopy pictures of **4** at pH 7.8 (A) and 8.6 (B) and **5** at pH 6.9 (C). Bar represents 100 nm.

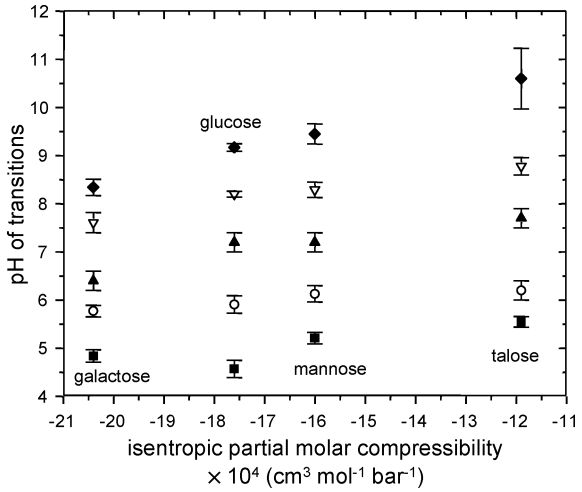

Figure 6. Plot of the pH of the transitions of **2**, **9**, **11**, and **12** as a function of the isentropic partial molar compressibility of the cyclic pyranosides from which the gemini surfactants are derived. Symbols have the same meaning as those in Figure 3.

area. Indeed, when considering the phase behavior of **7** and **8** only transitions associated with low packing parameters are observed.

Contrary to **2**, **5**, and **6,** the inverted phases formed from **7** and **8** do not adsorb hydroxide ions.

Effects of Carbohydrate Stereochemistry. The second issue to address for this series of gemini surfactants is the influence of the (reduced) carbohydrate stereochemistry on the pH of the transitions. This has been performed first for the gemini surfactants with identical *n*-hexyl spacers, but carrying different (reduced) carbohydrate head groups. For this purpose the carbohydrates glucose, mannose, galactose, and talose have been selected as the nonreduced carbohydrates since they possess the largest possible variety of solution properties that can be observed for carbohydrates (vide infra).[19−21]

Gemini **9** has been studied before,[12] but that was mainly to determine binding constants for protons and hydroxide ions. Although the same sample preparation was employed for all compounds, solutions containing **12** showed multilamellar vesicles instead of the usually observed unilamellar vesicles, but similar transitions could be identified (Supporting Information).

In Figure 6 the pH of the transitions are plotted for **2**, **9**, **11**, and **12** versus the isentropic partial molar compressibility of the corresponding cyclic pyranosides. This parameter was chosen because (1) it can be measured relatively unambiguously (compared to, for example, hydration numbers) and (2) isentropic partial molar compressibility values can be directly related to the properties of the carbohydrate hydration layer. Previous work has established that the surface hydration layers have an important influence on both the phase transitions and the hydroxide-ion binding.[22]

SCHEME 2: Fisher Projection of Glucose (A); Mode of Reduced Glucose Incorporation into the Gemini Surfactant Structure (B)[a]

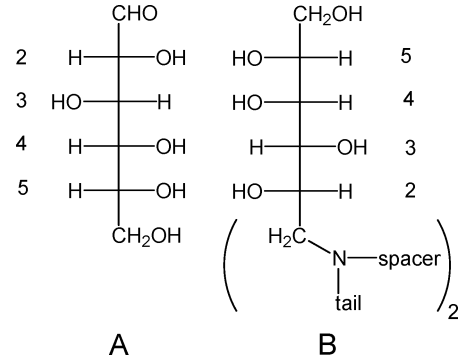

[a] The number corresponds to the number of the carbon atom. Following the numbering, the stereochemistry is then *R*,*S*,*R*,*R* from the second to fifth position.

The isentropic partial molar compressibility contains information about how solutes fit into the water hydrogen-bond network.[19,20] Assuming that the carbohydrate molecules are incompressible, compressibilities for solutions containing carbohydrates therefore yield information about the hydration layer of the carbohydrate. Solutes with values close to that of water (8.17×10^{-4} cm^3 mol^{-1} bar^{-1}) fit well into the hydrogen-bond structure of water since the hydration layer is similar to that of bulk water. By contrast, the hydration layer around ions has an isentropic partial molar compressibility between -50 and -30 $\times 10^{-4}$ cm^3 mol^{-1} bar^{-1}, depending on the hydration properties of the particular ion. The isentropic partial molar compressibility of hydrophobic solutes also has a negative sign. Hence, isentropic partial molar compressibilities do not yield information about the type of hydration, but only suggest compatibility of the hydration layer with the hydrogen-bond network of bulk water.

The pyranoside that disturbs the three-dimensional hydrogen bond network of bulk water the least is talose, the one that disturbs it the most is galactose.[21] Glucose and mannose are intermediate cases. In the literature this has primarily been attributed to the stereochemistry at the 2 and 4 position (Scheme 2) of the pyranoside ring and the resulting distances between the corresponding oxygen atoms, either favoring intramolecular hydrogen bonding or disfavoring it.[21]

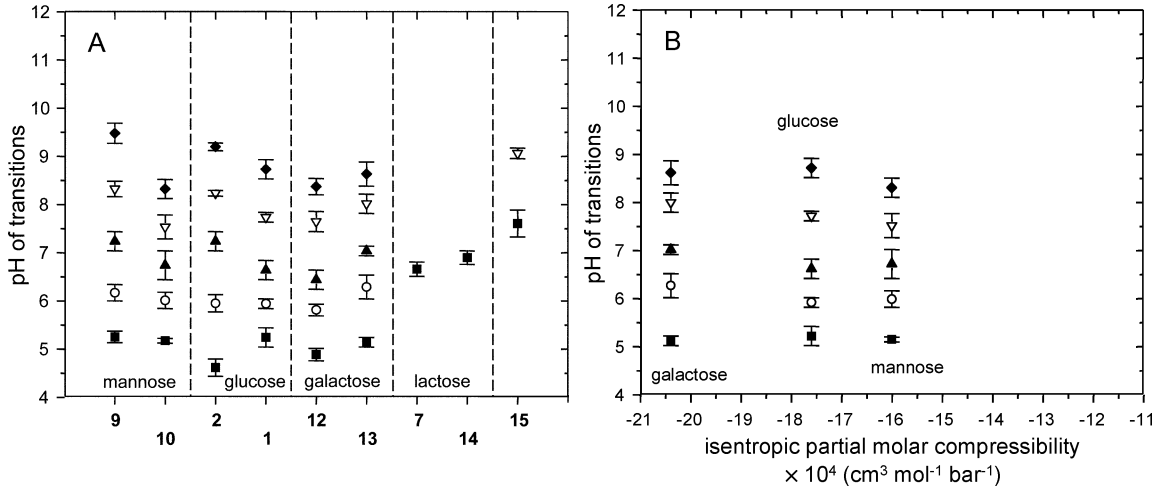

Figure 7. Plot of the pH of the transitions as a function of the spacer (A) and isentropic partial molar compressibility (B) of the cyclic pyranosides from which the gemini surfactants are derived. Symbols have the same meaning as those in Figure 3.

The gemini surfactants under study contain the (reduced) linear counterparts of the cyclic carbohydrates. Since linear carbohydrates have significantly more reorientational freedom than cyclic carbohydrates, the isentropic partial molar compressibility of the carbohydrates in the gemini surfactants may deviate substantially. Nevertheless, we speculate that although the absolute values of the isentropic partial molar compressibilities will not be reliable, at least the trend may be correct. Indeed, as can be seen in Figure 6, the pH of the transitions generally increases with decreasing isentropic partial molar compressibility. The low pH transitions are less affected than the transitions that occur at higher pH. For the latter transitions, the smallest increase going from **12** (galactose) to **11** (talose) is about 0.9 pH units, whereas the largest increase is about 2.3 pH units.

As before, this leads to the conclusion that (1) the degree of protonation is not affected by the carbohydrate stereochemistry and that (2) at high degrees of protonation phase transitions are mainly determined by the presence of charged nitrogen atoms and not so much by the carbohydrate stereochemistry. For the low surface potential transitions, the changes in the pH of redispersion are particularly intriguing since the ability to adsorb hydroxide ions has been linked to the requirement of ordering of water molecules in the first few hydration layers along the surface of the vesicular plane.[8,22] Hence, the gemini surfactant build from (reduced) talose that disturbs the ordering of bulk water the least shows the weakest ability of hydroxide-ion adsorption. On the contrary, **12**, which contains galactose, is the best at adsorbing hydroxide ions (vide infra).

Effects of the Nature of the Spacer. Previously the effect of the nature of the spacer on the phase behavior has been studied briefly for **10** ($-(EO)_2-(CH_2)_2-$ spacer) and **9** ($-(CH_2)_6-$ spacer).[12] Despite the large difference in hydrophobicity of these spacers, both gemini surfactants display the same phase behavior (including adsorption of hydroxide ions) with transitions that are similar for both surfactants at acidic pH (Figure 7A). At more basic pH, the pH of the transitions are lowered by more than one pH unit going to the hydrophilic spacer. This larger effect of the spacer near charge neutrality of the vesicles is not unexpected (vide supra). The results at basic pH prompted us to extend this structural variation to a number of other (reduced) carbohydrate head groups, including glucose, galactose and lactose. The pHs of most transitions are only weakly affected. Roughly, for the glucose and mannose head group the pH of the transitions are lowered going to the hydrophilic spacer, but for galactose and lactose they are increased. Lacking a clear trend upon a change in spacer hydrophilicity, again the data was plotted against the isentropic partial molar compressibility (Figure 7B) similar as to what was done in Figure 6. Whereas for the hydrophobic spacer the pH of the transitions increases upon an increasing fit into the water structure of the (reduced) carbohydrate head group, for the hydrophilic spacer the transitions are only slightly affected. This implies that the effect of the hydrophilic spacer, contrary to the effect the hydrophobic spacer, is more important than the carbohydrate stereochemistry.

Effects of Carbohydrate and Spacer Modifications. The degree of protonation of the nitrogen atoms of the gemini surfactants is determined by a number of parameters.[23] First of all, the inter- and intramolecular N−N distance play an important role. This topic has been addressed in some detail recently.[9] For spacers longer than six carbon atoms, the intermolecular N−N distance in the aggregate is more important than the intramolecular N−N distance in a single amphiphilic molecule. Hence, the difference in length between the $-(CH_2)_6-$ and $-(EO)_2-(CH_2)_2-$ spacer does not account for differences in the degree of protonation. Second, the degree of protonation is affected by the local hydrogen bonding in the hydration shell. Inversely, protonation affects the local water hydrogen-bond structure. Other factors that affect the local water structure can be the size of the carbohydrate moiety, its stereochemistry and the nature of the spacer. Variation of these parameters shows that the pH of the transition from spherical micelles toward structures with lower surface curvature is in all cases rather constant. This suggests that in a rather narrow pH range (around pH 5) the same packing parameter is achieved independent of these structural variations. Considering that neither the hydrophobic volume nor the length of the alkyl tail is varied, the mean cross sectional head group area must also be constant.[24] This leads to the conclusion that in this pH range (1) a similar degree of protonation is achieved at a particular pH value and (2) that the charged nitrogen atoms mainly determine the mean cross sectional head group area. Alternatively, one could argue that a change in mean cross sectional head group area due to structural variation is counteracted by a change in the degree of protonation, leading to a constant mean cross sectional head group area. However, considering the generality of the constant pH of the low pH transitions we find this unlikely. Therefore, at high degrees of protonation neither the size of the carbohydrate, nor the stereochemistry nor the nature of the spacer affect

the degree of protonation significantly. The only exceptions arise when the size of the carbohydrate head group is increased from 6 to 12 carbon atoms, or when the spacer is large and hydrophilic (**15**; Figure 7A; in this case the spacer acts in part as a head group).

At higher (basic) pH, and hence lower surface potential, the pH of some of the transitions and the nature of the transitions are affected by structural variations. For gemini surfactants with a hydrophobic spacer a change in the size of the carbohydrate head group affects the type of aggregates formed. At basic pH, inverted phases ($P > 1$) are more easily formed upon decreasing head group size. Hence, the carbohydrate group affects the surface area. However, this does not necessarily mean that the degree of protonation at constant pH is also affected. Unfortunately, on the basis of the present data no conclusions on the degree of protonation can be drawn.

On the contrary, changes in the degree of protonation at constant pH are observed when the carbohydrate stereochemistry is varied for gemini surfactants with a hydrophobic spacer. For these gemini surfactants the types of transitions are unaffected, but the pH values of the transitions are. However, for gemini surfactants with a hydrophilic spacer, the effect of carbohydrate stereochemistry is not observed. This means that carbohydrate stereochemistry, in combination with a hydrophobic spacer, determines the headgroup area due to different hydration effects, while in combination with a hydrophilic spacer the carbohydrate stereochemistry is less important.

Special attention has to be paid to the adsorption of hydroxide ions. Despite the differences in hydration for hydrophobic and hydrophilic spacers and their dependence on carbohydrate stereochemistry, at basic pH hydroxide ions are adsorbed at the interface of vesicles formed from all the present gemini surfactants. In addition, the adsorption of hydroxide ions has been observed to occur to several rather different nonionic (spherical) particles, including oil droplets formed from the gemini surfactants.[8,25−30] Recently, MD simulations have shown that adsorption to hydrophobic surfaces is unique for hydroxide ions and probably a result of the preferential orientation of water molecules in the first two water layers away from the hydrophobic surface (i.e., adsorption is a result of water orientation).[22]

In addition, vibrational sum frequency spectroscopy (VSFS) has been employed to study the interface between water and organic solvents and vapor in the presence and absence of nonionic surfactants.[31,32] It was found that the water structure at these hydrophobic interfaces is distinctly different from each other.[33] Nevertheless, adsorption of hydroxide ions occurs to all of these interfaces.[26] Although VSFS experiments require flat interfaces and that in other studies curved interfaces of oil droplets and bilayered aggregates are used the general phenomena is the same, i.e., they all adsorb hydroxide ions. Therefore, we anticipate that adsorption of hydroxide ions to these interfaces does not require a specific type of hydration (e.g., hydrophobic hydration). Instead, we anticipate that only regular ordering of water molecules in the first few water layers along the surface of a (nearly) flat interface is required for adsorption of hydroxide ions. The presence of charges at the interface creates irregularities in this ordering along the surface, and consequently, those surfaces do not adsorb hydroxide ions.[12] For example, in the presence of phospholipids no hydroxide ions are adsorbed at the water/vapor interface.[34]

Conclusions

The effects of the size of the head group, carbohydrate stereochemistry and the nature of the spacer have been examined for a series of (reduced) carbohydrate-based gemini surfactants that display a rich pH-dependent phase behavior. For gemini surfactants, bearing a head group derived from a monosaccharide, at near neutral pH vesicles are formed. They undergo transitions toward wormlike micelles and spherical micelles upon a lowering in pH as can be explained in terms of a decrease in the packing parameter. Upon increasing the pH of a vesicular solution flocculation is observed. However, upon a further pH increase redispersion is observed leading to vesicles of the same size distribution which are stabilized by adsorption of hydroxide ions. Our results suggest that hydrophobic hydration of the vesicular surface is not a prerequisite for the specific ordering of the water molecules as required for hydroxide-ion binding.

For almost all gemini surfactants the lowest pH transition, i.e., the transition to spherical micelles from aggregates with lower curvature, is not so much affected by a change in head group or spacer. Hence, the degree of protonation is similar for all the gemini surfactants and the surface area is mainly determined by the charged nitrogen atoms. Gemini surfactants containing a disaccharide head group or a long hydrophilic spacer are exceptions.

At lower degrees of protonation, however, the type of head group contributes significantly to the phase transitions and the pH of these transitions. Upon decreasing head group size, partial deprotonation leads readily to a packing parameter that is larger than one. As a result, inverted phases are formed. Therefore, the surface area of gemini surfactants at lower degrees of protonation is mainly determined by the size of the carbohydrate moiety. The gemini surfactants with the smallest head groups are liquids at room temperature and they cannot maintain their inverted structure, leading to oil droplet formation.

Variation of the carbohydrate stereochemistry does not lead to different aggregate morphologies. However, in combination with a hydrophobic spacer, the pH values of the transitions increase upon an increasing fit into the water structure of the (reduced) carbohydrate that is built into the gemini surfactant. For a hydrophilic spacer, this is not the case since the hydrophilic spacer has a strong influence on the hydration layer.

Acknowledgment. J.E.K. acknowledges the National Research School Combination Catalysis for financial support.

Supporting Information Available: Static and dynamic light scattering data of **3**−**5** and **7**−**15**. Cryo-electron microscopy pictures of **2**, **3**, **7**, and **12**. This material is available free of charge via the Internet at http://pubs.acs.org.

References and Notes

(1) Zana, R. *Adv. Colloid Interface Sci.* **2002**, *97*, 205−253.
(2) Bunton, C. A.; Robinson, L.; Schaak, J.; Stam, M. F. *J. Org. Chem.* **1971**, *36*, 2346−2350.
(3) Zana, R.; Talmon, Y. *Nature* **1993**, *362*, 228−230.
(4) Wang, X. Y.; Wang, J. B.; Wang, Y. L.; Ye, J. P.; Yan, H. K.; Thomas, R. K. *J. Phys. Chem. B* **2003**, *107*, 11428−11432.
(5) Yoshimura, T.; Nyuta, K.; Esumi, K. *Langmuir* **2005**, *21*, 2682−2688.
(6) Bergsma, M.; Fielden, M. L.; Engberts, J. B. F. N. *J. Colloid Interface Sci.* **2001**, *243*, 491−495.
(7) Johnsson, M.; Engberts, J. B. F. N. *J. Phys. Org. Chem.* **2004**, *17*, 934−944.
(8) Klijn, J. E.; Scarzello, M.; Stuart, M. C. A.; Wagenaar, A.; Engberts, J. B. F. N. *Org. Biomol. Chem.* **2006**, *4*, 3569−3570.
(9) Klijn, J. E.; Stuart, M. C. A.; Scarzello, M.; Wagenaar, A.; Engberts, J. B. F. N. *J. Phys. Chem. B* **2006**, *110*, 21694−21700.
(10) Fielden, M. L.; Perrin, C.; Kremer, A.; Bergsma, M.; Stuart, M. C.; Camilleri, P.; Engberts, J. B. F. N. *Eur. J. Biochem.* **2001**, *268*, 1269−1279.
(11) Wasungu, L.; Scarzello, M.; van Dam, G.; Molema, G.; Wagenaar, A.; Engberts, J. B. F. N.; Hoekstra, D. *J. Mol. Med.* **2006**, *84*, 774−784.

(12) Johnsson, M.; Wagenaar, A.; Stuart, M. C. A.; Engberts, J. B. F. N. *Langmuir* **2003**, *19*, 4609−4618.

(13) Wagenaar, A.; Engberts, J. B. F. N. Submitted for publication.

(14) Israelachvili, J. N.; Mitchell, D. J.; Ninham, B. W. *J. Chem. Soc., Faraday Trans. 2* **1976**, *72*, 1525−1568.

(15) Johnsson, M.; Wagenaar, A.; Engberts, J. B. F. N. *J. Am. Chem. Soc.* **2003**, *125*, 757−760.

(16) Siegel, D. P.; Green, W. J.; Talmon, Y. *Biophys. J.* **1994**, *66*, 402−414.

(17) Gustafsson, J.; Nylander, T.; Almgren, M.; Ljusberg-Wahren, H. *J. Colloid Interface Sci.* **1999**, *211*, 326−335.

(18) As will be discussed later on, it can't be excluded that the decreasing size of the carbohydrate moiety is counteracted by an increase in the degree of protonation leading to a constant mean cross sectional head group area, but this seems unlikely.

(19) Høiland, H.; Holvik, H. *J. Sol. Chem.* **1978**, *7*, 587−596.

(20) Galema, S. A.; Engberts, J. B. F. N.; Høiland, H.; Forland, G. M. *J. Phys. Chem.* **1993**, *97*, 6885−6889.

(21) Galema, S. A.; Howard, E.; Engberts, J. B. F. N.; Grigera, J. R. *Carbohydr. Res.* **1994**, *265*, 215−225.

(22) Zangi, R.; Engberts, J. B. F. N. *J. Am. Chem. Soc.* **2005**, *127*, 2272−2276.

(23) For simplicity, the nature of the aggregate (micelle, vesicle, etc.) will be left of the discussion.

(24) Previously it has been concluded that a spacer with six carbon atoms does not fold back into the hydrophobic domain significantly (ref 9)

(25) Graciaa, A.; Morel, G.; Saulner, P.; Lachaise, J.; Schechter, R. S. *J. Colloid Interface Sci.* **1995**, *172*, 131−136.

(26) Marinova, K. G.; Alargova, R. G.; Denkov, N. D.; Velev, O. D.; Petsev, D. N.; Ivanov, I. B.; Borwankar, R. P. *Langmuir* **1996**, *12*, 2045−2051.

(27) Zheng, L. Q.; Shui, L. L.; Shen, Q.; LI, G. Z.; Baba, T.; Minamikawa, H.; Hato, M. *Colloids Surf. A* **2002**, *207*, 215−221.

(28) Pashley, R. M. *J. Phys. Chem. B* **2003**, *107*, 1714−1720.

(29) Maeda, N.; Rosenberg, K. J.; Israelachvili, J. N.; Pashley, R. M. *Langmuir* **2004**, *20*, 3129−3137.

(30) Beattie, J. K.; Djerdjev, A. M.; Franks, G. V.; Warr, G. G. *J. Phys. Chem. B* **2005**, *109*, 15675−15676.

(31) Richmond, G. L. *Chem. Rev.* **2002**, *102*, 2693−2724.

(32) Tyrode, E.; Johnson, C. M.; Kumpulainen, A. J.; Rutland, M. W.; Claesson, P. M. *J. Am. Chem. Soc.* **2005**, *127*, 16848−16859.

(33) Scatena, L. F.; Richmond, G. L. *J. Phys. Chem. B* **2001**, *105*, 11240−11250.

(34) Watry, M. R.; Tarbuck, T. L.; Richmond, G. L. *J. Phys. Chem. B* **2003**, *107*, 512−518.